

Article

Not peer-reviewed version

A Modification to the Remotely Sensed Active Layer Thickness (ReSALT) Algorithm to have Self-Consistency

[Jatin Mathur](#)^{*} and Suhani Dalal

Posted Date: 7 December 2023

doi: 10.20944/preprints202312.0500.v1

Keywords: synthetic aperture radar; interferometric synthetic aperture radar; permafrost thaw; climate change



Preprints.org is a free multidiscipline platform providing preprint service that is dedicated to making early versions of research outputs permanently available and citable. Preprints posted at Preprints.org appear in Web of Science, Crossref, Google Scholar, Scilit, Europe PMC.

Copyright: This is an open access article distributed under the Creative Commons Attribution License which permits unrestricted use, distribution, and reproduction in any medium, provided the original work is properly cited.

Article

A Modification to the Remotely Sensed Active Layer Thickness (ReSALT) Algorithm to Have Self-Consistency

Jatin Mathur * and Suhani Dalal

suhanidalal8@gmail.com

* Correspondence: jatin.mathur25@gmail.com

Abstract: Permafrost thaw is an important aspect of Earth's carbon cycles. Initial estimates suggest that permafrost thaw could contribute anywhere between 20 to 500 Gt of CO₂-eq by 2100. These estimates are all fundamentally centered around one number: active layer thickness (ALT). The deeper the ALT, the more emissions. Unfortunately, ALT is a highly spatially heterogeneous number and determined by numerous thermal, soil hydrology, and geomorphological effects. The remotely sensed active layer thickness (ReSALT) algorithm was introduced in 2010 to provide scientists a way to model ALT heterogeneously at meter-scale resolution. However, upon inspection, this work shows that ReSALT's modelling approach is self-inconsistent. This work then introduces SCReSALT (Self-Consistent ReSALT) to solve that problem. SCReSALT is conceptually simple, physics-based, self-consistent, and makes no approximations. Experimental comparisons to a past study in Utqiagvik (formerly Barrow), Alaska show significant improvement and suggest that SCReSALT should replace ReSALT.

Keywords: synthetic aperture radar; interferometric synthetic aperture radar; permafrost thaw; climate change

1. Introduction

Climate forecasting studies estimate that permafrost thaw could contribute anywhere between 20 to 500 Gt of CO₂-eq by 2100 ([1–4]). These estimates varied in the phenomenon they modeled, how that phenomenon was modeled, and assumptions of warming trends, therefore explaining the wide range of predictions. Regardless of these differences, a crucial variable in all forecasts is the active layer thickness (ALT), which describes the topmost layer of permafrost subject to annual freeze and thaw. Warmer temperatures lead to deeper active layers. Organic carbon is distributed throughout the soil column, meaning deeper active layers permit microbacteria to process more carbon and emit more greenhouse gases. For more background on permafrost carbon cycles, the reader is referred to [5].

2. Background

2.1. ReSALT Description

The remotely sensed active layer thickness (ReSALT) algorithm was introduced to model ALT with broad spatial coverage while preserving heterogeneous predictive power [6]. Without remote sensing, our understanding of permafrost thaw is constrained to sparse in-situ observations. Given the vast extent of permafrost, it would be incredibly useful if remote sensing could accurately monitor ALT. ReSALT leverages a technique known as interferometric synthetic aperture radar (InSAR) to create its predictions. For background information on InSAR, the reader is referred to [7]. For the purpose of analysis in this paper, an InSAR measurement should be thought of as having three properties: i) the date of the reference SAR acquisition, ii) the date of the secondary SAR acquisition, and iii) an

image containing ground subsidence¹ per pixel. Specifically, if the ground position is measured as δ in an unchanging, earth-centered reference frame and the positive direction points towards the Earth's center, then the image will consist of $D = \delta_{reference} - \delta_{secondary}$ per pixel.

ReSALT has been used in several studies since its conception, such as in [6,8–10]. While it has demonstrated promising results, there is room for improvement. For example, the Permafrost Dynamics Observatory project reported a root-mean-square-error (RMSE) of 15.18 cm in ReSALT predicted vs in-situ ALTs [10]. The in-situ data had an average ALT of around 55 cm, making the RMSE significantly large with respect to the unit of measure. This large error served as motivation for this paper.

ReSALT is based on two main phenomenon. The first is ALT is proportional to \sqrt{ADDT} , where *ADDT* stands for Accumulated Degree Days of Thaw. This is the well-known Stefan Equation and is shown in (1).

$$h(t_i) = N\sqrt{ADDT(t_i)} \quad (1)$$

where N is a proportionality factor. This is derived in Appendix A. The second is that soil is fully saturated, meaning all pore space is filled with water. Consequently, when ice thaws into liquid water, the amount of volume reduces, which leads to a subsidence of the ground. This is shown visually in Figure 1 and captured mathematically in (2).

$$\delta(t_i) = \frac{p_w - p_i}{p_i} \int_0^{h(t_i)} PSdh = f(h(t_i)) \quad (2)$$

where p_w is the density of water, p_i is the density of ice, P is the soil porosity, and S is the soil saturation. The integral captures the volumetric water content. The ratio $\frac{p_w - p_i}{p_i}$ describes the difference in volume height when the ice phase transitions to liquid water per unit volume of ice.² We can then compute the difference in ground height by multiplying the two quantities, therefore arriving at (2). f is introduced as a convenience to compute subsidence from ALT.

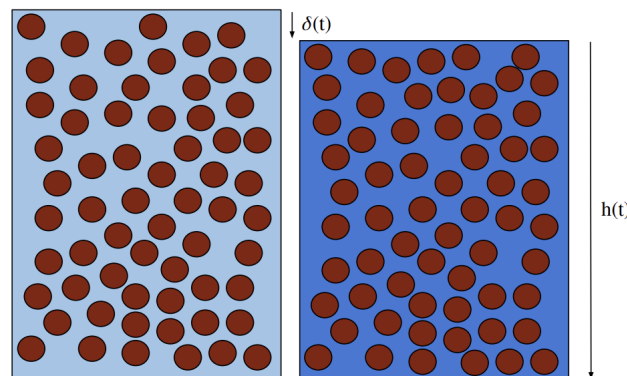


Figure 1. The left box shows the soil column during winter when all water is frozen. The right box shows the soil column during summer when water is thawed up to the ALT. Subsidence δ occurs because ice takes up more volume than water for the same mass. Hence, under the assumptions of no water loss and a fully saturated soil, we observe ground subsidence. Note that $h(t)$ is typically measured with respect to the ground at the time of measurement. δ is typically not measured.

¹ For the remainder of this paper, ground subsidence refers to the downwards motion of the ground and is a measure of distance. If the ground shifts down, subsidence is a positive number. If the ground shifts up, subsidence is negative.

² [10] argues convincingly that the ReSALT formulation only works when $S = 1$. If $S < 1$, some open pore space will be filled by freeze/thaw before the ground subsides. At a critical threshold (characterized by the densities of liquid water and ice), freeze/thaw might lead to no ground subsidence. So, we assume $S = 1$.

Any particular InSAR image contains subsidence difference $D = \delta(t_i) - \delta(t_j)$. Temperature is typically known at a coarse resolution. Hence, ReSALT strives to find a way to relate these two quantities, and ultimately retrieve $h(t)$. It does so by posing the following least-squares inversion problem:

$$\begin{bmatrix} D_1 \\ \vdots \\ D_N \end{bmatrix} = \begin{bmatrix} t_{2,1} - t_{1,1} & \sqrt{ADDT_{2,1}} - \sqrt{ADDT_{1,1}} \\ \vdots & \vdots \\ t_{2,N} - t_{1,N} & \sqrt{ADDT_{2,N}} - \sqrt{ADDT_{1,N}} \end{bmatrix} \begin{bmatrix} R \\ E \end{bmatrix} \quad (3)$$

where D_i is the measured subsidence difference in the i th interferogram, $t_{2,i}$ and $t_{1,i}$ describe the times of the two SAR acquisitions that were used to create the i th interferogram, and $ADDT_{2,i}$ and $ADDT_{1,i}$ describe the $ADDT$'s for $t_{2,i}$ and $t_{1,i}$. Note that all D_i refer to the same geographic location, but may differ in pixel location from image to image. R and E are the unknown variables and are solved for. R captures a long-term subsidence trend. More information can be found in [6,11]. E captures the relationship between \sqrt{ADDT} and subsidence difference, which can then be used to identify subsidence at any arbitrary time t via:

$$\delta(t) = E\sqrt{ADDT(t)} \quad (4)$$

Then, (2) can be inverted to obtain $h(t)$. More details on ReSALT's derivation are shown in Appendix B.

2.2. ReSALT Inconsistency Description

In (4), we see that subsidence difference is modeled as proportional to \sqrt{ADDT} . Using (1) and (2), we can see that this only happens when P is constant with depth. Hence, any application of ReSALT that uses a non-constant porosity model is self-inconsistent. Examples of self-inconsistent applications of ReSALT are [8] and [9], which use the "mixed soil model" shown later in this paper.

3. Method

The fundamental problem is that we only measure $ADDT$ and subsidence difference $D = \delta_{t_i} - \delta_{t_j}$, but we know no relationship between the two. We will first demonstrate a simple way to solve this problem for a practical soil moisture model. Then, we will more rigorously analyze the proposed method to understand its properties.

If we ignore R , we can see that the correct inversion LHS (left-hand side) for (3) is ALT difference:

$$h(t_i) - h(t_j) = \sqrt{\frac{2k_p}{p_p L}} \left(\sqrt{ADDT(t_i)} - \sqrt{ADDT(t_j)} \right) \quad (5)$$

To see if subsidence difference can be related to ALT difference, we analyze (1) as a ratio:

$$\frac{h(t_i)}{h(t_j)} = \sqrt{\frac{ADDT(t_i)}{ADDT(t_j)}} \quad (6)$$

$$h(t_i) = h(t_j) \sqrt{\frac{ADDT(t_i)}{ADDT(t_j)}} \quad (7)$$

Next, we fix some ratio $Q = \sqrt{\frac{ADDT(t_i)}{ADDT(t_j)}}$, create a list of h_{t_j} on some large interval of candidate ALTs, generate corresponding h_{t_i} use (7) to calculate the corresponding subsidences for each h_{t_j} and h_{t_i} , and then plot ALT differences and corresponding subsidence differences. See Figure 2 for examples of this plot for two soil porosity models. Each of these models is explained explicitly in [8]. As shown via a "horizontal line test," a particular subsidence difference can always be directly mapped to an ALT

difference with zero ambiguity. Intuitively, this is because (7) enables multiplicative growth of h_{t_i} with respect to h_{t_j} . Consequently, we would hope that (2) enables subsidence difference to grow strictly monotonically. Of course, there is no guarantee that this always will be the case. A counterexample is discussed in Section 3.1.

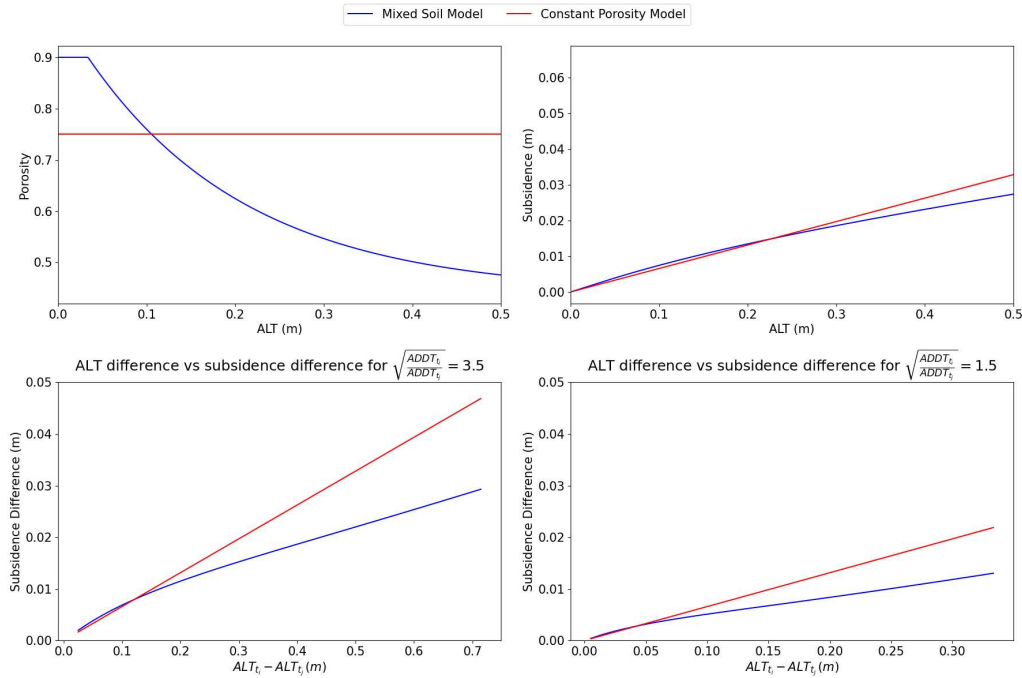


Figure 2. The top-left and top-right charts show porosity and ground subsidence as a function of ALT for two soil models. The “mixed soil model” is described in detail in [8]. The bottom-left and bottom-right charts show how ALT difference relates to subsidence difference for a particular Q ratio. The two given soil porosity models happen to exhibit behavior such that a larger increase in ALT leads to larger subsidence differences. Hence, a subsidence difference can be mapped directly to an ALT difference (and also, as it turns out, exact knowledge of the ALT pair). The bottom-right image also demonstrates the effect of Q on the robustness of the method. For the constant porosity model, there is no effect because ALT difference is linearly related to subsidence difference (independent of $ADDT$). For the “mixed soil model,” we can see that the slope is higher, making it easier to identify a particular ALT difference from a given subsidence difference. This is expected, because larger Q ratios make the ALT pair sampled at smaller ALT values (for the same ALT difference), which exhibits larger subsidence gradient as shown in the top-right plot.

This method is summarized Algorithm 1. We can now rewrite (3) as:

$$\begin{bmatrix} y_i \\ \vdots \\ y_N \end{bmatrix} = \begin{bmatrix} \sqrt{ADDT_{2,1}} - \sqrt{ADDT_{1,1}} \\ \vdots \\ \sqrt{ADDT_{2,N}} - \sqrt{ADDT_{1,N}} \end{bmatrix} [A] \quad (8)$$

where y_i is the best-matching ALT difference reported for each D_i via Algorithm 1. This now forms a self-consistent modelling of thaw, temperature, and ground subsidence. Hence, we call this new method SCReSALT (Self-Consistent ReSALT). Least-squares inversion gives the best A , which can then be used to find ALT at any point in the thaw season:

$$h(t) = A\sqrt{ADDT(t)} \quad (9)$$

Algorithm 1 Self-Consistent ReSALT LHS Retrieval

Require: $Q = \sqrt{\frac{ADDT_i}{ADDT_j}}$
Require: $D =$ measured subsidence difference

- 1: $N \leftarrow$ number of samples
- 2: $L \leftarrow$ lower end possible ALTs
- 3: $U \leftarrow$ upper end possible ALTs
- 4: $step \leftarrow \frac{U-L}{N-1}$ ▷ Calculate step size for linear spacing
- 5: **for** $k = 1 \rightarrow N$ **do**
- 6: $h_{k,j} \leftarrow L + (k-1) \times step$
- 7: $h_{k,i} \leftarrow h_{k,j} \times Q$
- 8: $y_k \leftarrow h_{k,i} - h_{k,j}$
- 9: $x_k \leftarrow f(h_{k,i}) - f(h_{k,j})$ ▷ See (2)
- 10: **end for**
- 11: $e \leftarrow$ small neighborhood in which a subsidence difference should be unique
- 12: **if not** check_unique(x, y, e) **then**
- 13: **raise** Error("x and y have non-unique matching.")
- 14: **end if**
- 15: Find k such that x_k is closest to D
- 16: **return** y_k

To extend the formulation to multiple years, we simply need to discount the long-term trend R from the measured subsidence difference D_i before following the above approach. ReSALT jointly inverts for R and E , but a self-consistent model cannot do that. So, we must find a way to estimate R independently of and prior to A . Thankfully, there are many ways around this. Two are discussed here.

- Form interferograms across multiple years at the start of thaw season, ideally when $ADDT = 0$ (and perhaps there is some tolerance on how large $ADDT$ can get before it affects the result due to seasonal subsidence). Any observed subsidence can be attributed to R . Compute the best-fit R that solves all $D_i = R(t_i - t_j)$.
- Compute an initial estimate of A by solving (8). A could be solved either per thaw season (which makes $R = 0$) or overall. Then, like the previous bullet point, form interferograms across multiple years at the start of thaw season and remove the subsidence contribution due to ALT. This is known because the subsidence contribution due to ALT can be written as: $D_{ALT,i} = f(A_{s_{2,i}} \sqrt{ADDT_{2,i}}) - f(A_{s_{1,i}} \sqrt{ADDT_{1,i}})$. Note $A_{s_{2,i}}$ denotes A for the thaw season in the 2nd SAR image in the i th interferogram. $A_{s_{1,i}}$ means the same for the 1st SAR image. Compute the best-fit R that solves all $D_i - D_{ALT,i} = R(t_i - t_j)$.

Once R is known, the multi-year problem can be solved using (8) but instead of giving Algorithm 1 the observed subsidence difference D_i , give it $D_i - R(t_i - t_j)$.

For completeness, it is worth noting that both ReSALT and SCReSALT do not need both SAR acquisitions to be precisely during the thaw season. One acquisition could be before the thaw season, in which case we can assume $ADDT \approx 0$ for that acquisition. Hence, any measured subsidence difference can be modeled as the true subsidence at that point. ReSALT can directly use (3). SCReSALT would need a slight modification because it operates using ratios. Algorithm 1 could be modified such that if $ADDT_{t_j} < \epsilon$, simply report $y = f^{-1}(\delta)$. Similarly, if $ADDT_{t_i} < \epsilon$, report $y = f^{-1}(-\delta)$. The sign change is because δ is the subsidence underwent when going from t_j to t_i . That is expected to be positive if $ADDT_{t_i} > ADDT_{t_j}$ and negative vice-versa.

3.1. SCReSALT Counterexample Discussion

A more rigorous analysis of SCReSALT is shown in Appendix C. It shows a counterexample with a realistic soil porosity model that does not meet the SCReSALT requirement. Some possible workarounds are described below, but we leave exploring them to future work.

- From multiple interferograms per year and obtain time-series measurements of subsidence difference. Attempt to interpolate the measurements onto an ALT difference vs subsidence difference graph and determine which ALT differences best explain the data.
- Make sure to get a SAR acquisition before the thaw season starts. This allows one to treat the subsidence difference as the true subsidence. Handling this is easy and was described earlier in this paper.
- Incorporating a prior on ALT difference might isolate a particular ALT difference as the most likely candidate.

4. Experiments

To assess the practical improvement of our method, we reproduce and benchmark against the results reported in [9]. [9] applies ReSALT to Utqiagvik (formerly Barrow), Alaska to predict ALT from 2006 to 2010. The paper uses data from the U1 CALM³ plot. It uses ALOS-PALSAR L-band data and generates interferograms using the ISCE2 framework⁴. The paper defines the χ^2 metric:

$$\chi^2 = \frac{(ALT_{pred} - ALT_{gt})^2}{e^2} \quad (10)$$

where e is the uncertainty in the measurement. In [9], $e = 7.9$ cm. If $\chi^2 < 1.0$, it is called a “great match.” If the ALT_{gt} is within the uncertainty of ALT_{pred} , it is called a “good match.” Otherwise, it is called a “bad match.” We have not described uncertainty analysis in this paper, but in brief one could compute uncertainty by assigning an uncertainty to each ReSALT/SCReSALT parameter and either analytically propagating that into an uncertainty in the prediction or more practically using numerical simulation to understand the distribution of predictions as a function of the modeling parameter distributions. Since this paper is primarily concerned with RMSE improvement, and uses χ^2 as a way to assess reproduction accuracy, we do not discuss uncertainty explicitly in this analysis. Instead, we take advantage of the fact that [9] states that the ReSALT uncertainty is roughly twice that of the measurement uncertainty. Hence, we use $e_{ReSALT} = e_{SCReSALT} = 15.8$ cm. This makes the “great match,” “good match,” and “bad match” categorizations directly comparable. Additionally, [9] uses the same “mixed soil model” from [8]. Further specifics (namely image calibration) on the reproduction are described in Appendix D. With those details explained, results are shown in Table 1.

Table 1. Comparison of ReSALT vs. SCReSALT performance. In each row, the best score is bolded. Note that SCReSALT was fit using just A , so for comparison we also report results for ReSALT fit using just E . Also, ReSALT reported invalid ALT predictions on 8 pixels and ReSALT with just E reported invalid ALT predictions on an additional 6 pixels. SCReSALT always reported valid ALT predictions. So, for fair comparison, we report results for SCReSALT under the subset of data with valid ALT predictions across both types of ReSALT. We also report SCReSALT results on the entire dataset for more direct comparison against the paper. The double vertical line denotes the separation.

Metric	ReSALT	ReSALT (just E)	SCReSALT (subset)	[9]	SCReSALT (all)
Avg χ^2	3.7835	4.0980	2.2432	2.5	2.0475
Great Match	0.4950	0.4851	0.5644	0.62	0.5913
Good Match	0.2079	0.1782	0.2475	0.26	0.2435
Bad Match	0.2970	0.3366	0.1881	0.12	0.1652
Bias (m)	-0.0480	-0.0343	0.0620	\approx 0.01	0.0522
Pearson R	0.1546	0.2118	0.3566	-	0.3917
RMSE (m)	0.1537	0.1599	0.1183	-	0.1130

³ CALM is a long-running program that collects data on permafrost thaw. Data can be accessed at <https://www2.gwu.edu/~calm/>

⁴ <https://github.com/isce-framework/isce2>

5. Discussion

As we can see in Table 1, the reproduced ReSALT had much worse results than in the original paper. Private correspondence and a review of the software with the authors of [9] suggested that the reproduction was most likely very similar. Also, it is worth noting that [10] reported similar RMSEs to the reproduced ReSALT (albeit for a broader set of CALM sites). For completeness, we show comparisons between the reproduced ReSALT, the original paper, and SCReSALT. Given that SCReSALT outperforms the original paper on the χ^2 metric, we take these results to mean SCReSALT outperforms ReSALT. Of course, this is to be expected. SCReSALT makes no approximations and can perfectly model the “mixed soil model” in a self-consistent way.

6. Conclusion

We present SCReSALT, a modification to ReSALT that enables self-consistency. SCReSALT makes no approximations and reduces to ReSALT under the right soil models. We also rigorously analyze SCReSALT’s requirements and identify a counterexample where the requirements are not met. We then describe possible workarounds but leave exploring that to future work. Experimentally, SCReSALT demonstrates significant improvement in predicting ALTs in Utqiagvik, Alaska. We recommend SCReSALT become a standard tool in permafrost thaw modelling.

Conflicts of Interest: The authors declare no conflicts of interest.

Appendix A. Stefan’s Equation Derivation

We first derive Stefan’s Equation to understand the relationship between temperature history and ground ice thaw. Figure A1 is provided to help visualize the relevant processes. We start with Fourier’s Law:

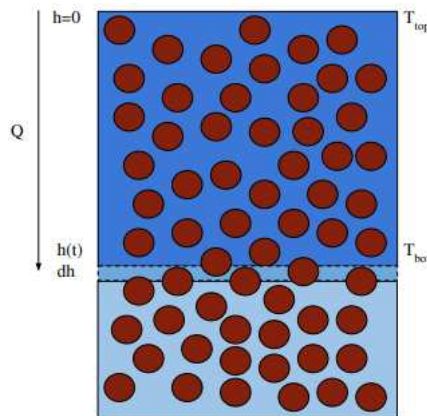


Figure A1. A diagram of a thawing soil column. h denotes the position of the thaw front. Q is the (uniform) heat flux induced by T_{top} and T_{bot} . T_{top} is the same as the temperature of the air. Brown circles denote soil particles. Anything that is not a soil particle is pore space. Note that any real soil would have a far more dense concentration of soil particles. Dark blue denotes liquid (thawed) water. Light blue denotes frozen (unthawed) water. In this diagram, we assume all pore space is filled with water. This does not have to be the case for Stefan’s equation to apply. A different bulk density ρ_p and latent heat of thaw L can capture the thaw dynamics of a variety of soil hydrology models.

$$Q = -k_p \frac{dT}{dh} \quad (11)$$

where Q is the heat per unit area per unit time, k_p is the thermal conductivity, T is temperature, and h defines the position of the thaw front. Note that both T and h are functions of time t . Assuming the temperature gradient is uniform throughout the column, we can write:

$$\frac{dT}{dh} = \frac{(T_{bot} - T_{top})}{h} \quad (12)$$

Next, we assume that all heat is absorbed as latent heat to facilitate phase change from ice to liquid water. Consequently, an infinitesimal change in thaw depth dh can be related to the amount of heat required to do so by:

$$H = p_p L dh \quad (13)$$

where H is the amount of heat per unit area required to advance the thaw front by dh , p_p is the bulk density of soil, and L is the latent heat of thawing. Differentiating with respect to time:

$$\frac{dH}{dt} = Q = p_p L \frac{dh}{dt} \quad (14)$$

Equating (14) and (12):

$$Q = -k_p \frac{T_{bot} - T_{top}}{h} = p_p L \frac{dh}{dt} \quad (15)$$

We now solve for h :

$$p_p L h dh = -k_p (T_{bot} - T_{top}) dt \quad (16)$$

$$\int_{h(t_1)}^{h(t_2)} p_p L h dh = \int_{t_1}^{t_2} -k_p (T_{bot} - T_{top}) dt \quad (17)$$

Since T_{bot} refers to the boundary of thawed/frozen soil, it is reasonable to assume $T_{bot} \approx 0$, in which case we can remove it from (17).

$$\int_{h(t_1)}^{h(t_2)} p_p L h dh = \int_{t_1}^{t_2} k_p (T_{top}) dt \quad (18)$$

Practically, once the thaw season begins $T_{top} > 0$. Since T_{top} is typically measured at daily basis (rather than continually), we can replace the right-hand side (RHS) with:

$$\int_{h(t_1)}^{h(t_2)} p_p L h dh = k_p (ADDT(t_2) - ADDT(t_1)) \quad (19)$$

where $ADDT$ stands for the Accumulated Degree Days of Thaw. It is a standard number used in permafrost literature and is calculated at any day t by summing the temperatures of all days preceding and including t . Now, looking at the left-hand side (LHS), if we assume p_p and L are constant with depth:

$$p_p L \int_{h(t_1)}^{h(t_2)} h dh = k_p (ADDT(t_2) - ADDT(t_1)) \quad (20)$$

$$p_p L \frac{1}{2} (h(t_2)^2 - h(t_1)^2) = k_p (ADDT(t_2) - ADDT(t_1)) \quad (21)$$

$$h(t_2)^2 - h(t_1)^2 = \frac{2k_p}{p_p L} (ADDT(t_2) - ADDT(t_1)) \quad (22)$$

At this point, we have derived Stefan's equation. It is the same as equation (A4) in [12]. Note that in this derivation, we used the opposite sign convention. We set $h = 0$ at the ground and make h increase with depth. [12] does the opposite, hence flipping some signs in the above equations.

Appendix B. ReSALT Derivation

We now present the derivation for ReSALT. First, we assume that thaw begins when $ADDT$ first exceeds $0^\circ\text{C}\text{-days}$.⁵ So, if t_s is the start of the thaw season, we know that $h(t_s) = 0$, $ADDT(t_s) = 0$.

⁵ [12] proposes that this is perhaps an erroneous assumption and suggests a different approach. However, we will not address that here.

Recall that (22) only applies for times within the thaw season, so that is why we need this assumption. We can then write the thaw depth at any time t_i :

$$h(t_i)^2 - h(t_s)^2 = \frac{2k_p}{p_p L} (ADDT(t_i) - ADDT(t_s)) \quad (23)$$

$$h(t_i)^2 = \frac{2k_p}{p_p L} ADDT(t_i) \quad (24)$$

$$h(t_i) = \sqrt{\frac{2k_p}{p_p L} ADDT(t_i)} \quad (25)$$

We have now derived (1). InSAR gives measurements of ground subsidence $D = \delta(t_i) - \delta(t_j)$ as determined by two SAR acquisitions at t_i and t_j . Most ReSALT methods model subsidence as (2). In general, P is not constant with depth. This means $\delta(t_i)$ is not linearly proportional to $h(t_i)$. However, because we only measure $ADDT$ and D , ReSALT strives to find a way to relate the two. To do so, it makes the assumption of constant porosity and therefore proportionality:

$$\delta(t_i) = \frac{p_w - p_i}{p_i} P h(t_i) \quad (26)$$

Substituting into (5):

$$\begin{aligned} \delta(t_i) - \delta(t_j) &= \frac{p_w - p_i}{p_i} P \sqrt{\frac{2k_p}{p_p L}} \\ &\times \left(\sqrt{ADDT(t_i)} - \sqrt{ADDT(t_j)} \right) \end{aligned} \quad (27)$$

For any InSAR measurement, we know $\delta(t_i) - \delta(t_j)$. We also know the times of the two SAR acquisitions, meaning we can determine $ADDT(t_i)$ and $ADDT(t_j)$. So, we could determine the coefficient $\frac{p_w - p_i}{p_i} P \sqrt{\frac{2k_p}{p_p L}}$. If we have multiple InSAR images, we can pose (27) as a least-squares inversion problem, leading to (3). Therefore, any use of (3) with a non-constant porosity model will be inconsistent.

Appendix C. SCReSALT Counterexample Analysis

We now conduct a more rigorous analysis of SCReSALT through which we derive a counterexample. The mathematical premise of SCReSALT can be stated as follows: Given an integrable⁶ function P for which $P(z) \in (0, 1)$, then for any ratio $Q = \sqrt{\frac{ADDT_i}{ADDT_j}} = \frac{h_{t_i}}{h_{t_j}} \neq 1$, $h_{t_i} - h_{t_j}$ can be uniquely identified by $\delta_{t_i} - \delta_{t_j}$ (following (2)). This can be restated as: if $f(Qz_1) - f(z_1) = f(Qz_2) - f(z_2)$, then SCReSALT requires $z_1 = z_2$. We know f is strictly increasing with z . We can write $P(z) = \frac{p_i}{p_w - p_i} f'(z)$. There are constraints on P , and hence constraints on f , but for simplicity we will at first ignore P and just consider f . To create a convincing failure case, we consider whether a range of Q can contradict the SCReSALT requirement. Mathematically, we consider two ratios Q_1, Q_2 and two points z_0, z_1 with the following property:

$$f(Q_1 z_0) - f(z_0) = f(Q_1 z_1) - f(z_1) \quad (28)$$

$$f(Q_2 z_0) - f(z_0) = f(Q_2 z_1) - f(z_1) \quad (29)$$

⁶ One might argue that a physically realizable P should be differentiable. We ignore that in the analysis presented in this paper, but it not hard to see that the example P given later could be made differentiable without changing the conclusion.

Taking the difference leads to:

$$f(Q_2 z_0) - f(Q_1 z_0) = f(Q_2 z_1) - f(Q_1 z_1) \quad (30)$$

If we assume $Q_2 = Q_1 + \Delta$, that Δ is small, and that f is locally linear around both z_0 and z_1 , we get:

$$m_0 \Delta z_0 = m_1 \Delta z_1 \quad (31)$$

$$m_0 z_0 = m_1 z_1 \quad (32)$$

where m_0 is the local linearity coefficient around z_0 and m_1 is the local linearity coefficient around z_1 . (32) might appear simple, but it contains our answer! This tells us that if $f'(z_0) = m_0$ and $f'(z_1) = m_1$, and they follow (32), then for some Q we will observe the same subsidence difference. If we extend the local linearity, we can extend the range of Q that lead to the same subsidence difference. Using this insight, we can devise a piecewise linear f that does not meet the SCReSALT requirement. We can use a quadratic function to fit the ends of the piecewise linear functions. As long as i) the values and derivatives match at the intersection points, ii) f is strictly increasing, and iii) a valid P can be constructed from f , we have met the requirements. An example is shown below:

$$f(z) = \begin{cases} 0.07z & \text{for } 0.01 \leq z < 0.04 \\ -z^2 + 0.15z - 0.0016 & \text{for } 0.04 \leq z < 0.07 \\ 0.01z + 0.0033 & \text{for } z \geq 0.07 \end{cases} \quad (33)$$

This example is scaled such that there is a valid corresponding P model. P can be generated by taking the derivative of each case and multiplying by $\frac{p_i}{p_w - p_i}$, as shown below.

$$P(z) = \begin{cases} 0.8 & \text{for } 0.01 \leq z < 0.04 \\ 11.431(-2z + 0.15) & \text{for } 0.04 \leq z < 0.07 \\ 0.1143 & \text{for } z \geq 0.07 \end{cases} \quad (34)$$

Both f and P are visualized in Figure A2, which demonstrates a potentially realistic soil porosity model that does not meet the SCReSALT requirement.

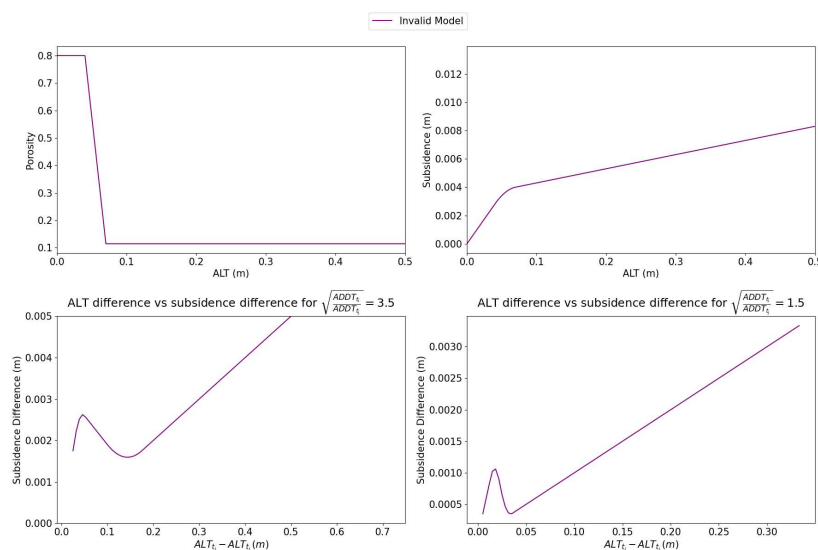


Figure A2. A diagram showing a physically realizable soil porosity model that fails the SCReSALT requirement. As shown in the bottom images, subsidence difference cannot necessarily be equated to an ALT difference.

Appendix D. Experiments Calibration Step

The paper uses node 61 of the U1 CALM⁷ plot as a reference or calibration node. In general, InSAR requires a calibration pixel where subsidence is known to calibrate the subsidence image. InSAR practitioners typically use a point in which subsidence is known, such as on gravel where it is assumed to be 0. In [9], no pixel had known subsidence, so they instead formulated (3) as “delta subsidence differences” with respect to node 61. After inversion, they calculated the subsidence of the calibration node by inputting its measured in-situ ALT into (2). They then corrected the best-fit E with a global offset that made the calibration node have the expected measured subsidence. This is actually problematic because the E that they compute is on a seasonal basis yet the calibrated subsidence measurement is at measurement time, which slightly predates the end-of-season. We do not correct this error, but simply take note of it here. An easy way to fix the error is to scale E by the \sqrt{ADDT} at measurement time, which would be a valid operation under ReSALT formulation (but not SCReSALT). SCReSALT handles the calibration node as follows:

1. SCReSALT is given the seasonal ALT of the calibration node as input. This is computed from the measured ALT and scaled by the end-of-season $ADDT$ according to (7).
2. For a particular InSAR image, the seasonal ALT of the calibration node is scaled at the time of the reference image and the secondary image using (7). (2) is then evaluated to get the expected subsidence in each image. The expected subsidence difference can then be computed. This is used to calibrate the subsidence difference reported in the InSAR image.
3. SCReSALT operates with the calibrated subsidence difference image.

To be clear, the steps listed above only need to be followed when the calibration node is itself subsiding. SCReSALT/ReSALT ultimately need an image in which subsidence difference is known.

References

1. Kevin Schaefer et al., “Amount and timing of permafrost carbon release in response to climate warming,” *Tellus B*, vol. 63, pp. 165–180, 2011.
2. Thomas Schneider von Deimling et al., “Observation-based modelling of permafrost carbon fluxes with accounting for deep carbon deposits and thermokarst activity,” *Biogeosciences*, vol. 12, pp. 3469–3488, 2015.
3. S. Ruiz, “\$41m audacious grant will tackle permafrost thaw,” *Woodwell Climate*, 2022, Available at: <https://www.woodwellclimate.org/41-million-grant-for-permafrost-thaw-monitoring/>. (Accessed: 1st November 2023).
4. “Carbon emissions from permafrost,” 50x30, 2023, Available at: <https://www.50x30.net/carbon-emissions-from-permafrost>. (Accessed: 1st November 2023).
5. K.R Miner et al., “Permafrost carbon emissions in a changing arctic,” *Nat Rev Earth Environ*, vol. 3, pp. 55–67, 2022.
6. Lin Liu et al., “Insar measurements of surface deformation over permafrost on the north slope of alaska,” *Journal of Geophysical Research*, vol. 115, 2010.
7. European Space Agency, “Insar principles: Guidelines for sar interferometry processing and interpretation,” Tech. Rep., ESA Publications ESTEC, February 2007.
8. Liu Liu et al., “Estimating 1992–2000 average active layer thickness on the alaskan north slope from remotely sensed surface subsidence,” *Journal of Geophysical Research: Earth Surface*, vol. 117, 2012.
9. Kevin Schaefer et al., “Remotely sensed active layer thickness (resalt) at barrow, alaska using interferometric synthetic aperture radar,” *Remote Sensing*, vol. 7, pp. 3735–3759, 2015.
10. Richard Chen et al., “Permafrost dynamics observatory (pdo): 2. joint retrieval of permafrost active layer thickness and soil moisture from l-band insar and p-band polsar,” *Earth and Space Science*, vol. 10, 2023.

⁷ CALM is a long-running program that collects and provides data on permafrost thaw. Data can be accessed at <https://www2.gwu.edu/~calm/>

11. F. Nixon and A. Taylor, "Regional active layer monitoring across the sporadic, discontinuous and continuous permafrost zones, mackenzie valley, northwestern canada," in *Proceedings of the 7th International Conference on Permafrost*, Yellowknife, Northwest Territories, Canada, 1998, International Permafrost Association, pp. 815–820.
12. Roger Michaelides et al., "Permafrost dynamics observatory—part i: Postprocessing and calibration methods of uavsar l-band insar data for seasonal subsidence estimation," *Earth and Space Science*, vol. 8, 2021.

Disclaimer/Publisher's Note: The statements, opinions and data contained in all publications are solely those of the individual author(s) and contributor(s) and not of MDPI and/or the editor(s). MDPI and/or the editor(s) disclaim responsibility for any injury to people or property resulting from any ideas, methods, instructions or products referred to in the content.